Letter

Coreless vortices as direct signature of chiral *d*-wave superconductivity

P. Holmvall and A. M. Black-Schaffer
Department of Physics and Astronomy, Uppsala University, Box 516, S-751 20, Uppsala, Sweden

(Received 16 December 2022; accepted 31 August 2023; published 15 September 2023)

Chiral *d*-wave superconductivity has been proposed in a number of different materials, but characteristic experimental fingerprints have been largely lacking. We show that quadruply quantized coreless vortices are prone to form and offer distinctive signatures of the chiral *d*-wave state in both the local density of states and the total magnetic moment. Their dissimilarity in positive versus negative magnetic fields leads to additional spontaneous symmetry breaking, producing clear evidence of time-reversal symmetry breaking, chiral superconductivity, and the Chern number.

DOI: 10.1103/PhysRevB.108.L100506

Exotic quantum states of matter continue to generate surprising phenomena. A prime example is chiral superconductors, where superconductivity is not only combined with nontrivial topology but also with spontaneous time-reversal symmetry breaking (TRSB) [1], causing many unconventional effects [2–6]. Most outstanding is the finite Chern number set by the order parameter winding, resulting in topologically protected chiral edge modes [7–14]. Early focus centered on chiral *p*-wave superconductivity [3,15] and its similarities to superfluidity in ^{3}He [2–6], while chiral *d*-wave superconductivity has more recently received significant attention due to proposals in a range of materials, including twisted bilayer cuprates [16,17], twisted bilayer graphene [18–26], Sn/Si(111) [27], SrPtAs [28–31], $LaPt_3P$ [32], Bi/Ni [33,34], and URu_2Si_2 [35–38]. Furthermore, chiral *d*-wave superconductivity was recently proposed as a platform to realize topological quantum computing [39–41].

Still, direct detection of both the superconducting pairing symmetry and topological invariants remain two of the most outstanding issues in physics. Consequently, undisputed discoveries of chiral superconductors have proven elusive. To make matters worse, recent studies have predicted that typical fingerprints, such as chiral edge currents and intrinsic orbital angular momentum (OAM), vanish for all pairing symmetries except *p*-wave [42–49], further complicating measurements. Indeed, while the chiral edge modes are topologically protected, their current and OAM are not [47,50,51]. In this paper, we set out to resolve this issue for chiral *d*-wave superconductors by identifying robust experimental bulk signatures in the form of distinctive vortex defects.

Vortices have been studied extensively in chiral *p*-wave superfluids [2–6], predicting vortex defects with no analog in conventional single-component systems. A prime example is the coreless vortex (CV) [52–56], which is multiply quantized and nonsingular with a finite superfluid order parameter everywhere. It has been sought experimentally in superfluid ^{3}He [55,57–65], with analogous states proposed theoretically in spin-triplet chiral *p*-wave [66–75] and multiband [76–79] superconductors. In comparison, however, vortices in spin-singlet chiral *d*-wave superconductors are not yet well understood, and it is not known how their higher Chern number influence vortex defects and their distinctive characteristics.

In this paper we establish that CVs can easily form, without spin-triplet or multiband pairing, in chiral *d*-wave superconductors. They appear as quadruply quantized vortex defects, consisting of a closed domain wall, stabilized by eight isolated fractional vortices, and leave signatures in the local density of states (LDOS) that are easily differentiable from Abrikosov vortices. Furthermore, the chirality causes inequivalent CVs in opposite magnetic field directions, leading to further spontaneous symmetry breaking of rotational and axial symmetries in only one field direction. We show that this generates prime, smoking-gun, signatures in both LDOS and total magnetic moment that differentiates not only TRSB and chiral superconductivity, but also the orbital ordering, thus directly accessing the Chern number. These signatures are measurable using well-established experimental techniques, including scanning tunneling spectroscopy (STS) and various magnetometry setups.

Model and method. We aim to study fundamental properties intrinsic to chiral *d*-wave superconductors, since such superconductivity has been proposed in a range of materials with widely different properties [14,16–41,80–84]. We thus consider a two-dimensional (2D) spin-singlet chiral *d*-wave superconductor. For simplicity, we focus here on a cylindrical Fermi surface in disk-shaped samples with radii $\mathcal{R} = 25\xi_0$, with superconducting coherence length $\xi_0 \equiv \hbar v_F/2\pi k_B T_c$, Planck constant $\hbar$, Fermi velocity v_F, Boltzmann constant k_B, and superconducting transition temperature T_c. We model clean systems with specular edges, and apply a perpendicular magnetic-flux density $\boldsymbol{B}_{ext} = B_{ext}\hat{\boldsymbol{z}}$ with homogeneous flux

$\Phi_{\rm ext} = B_{\rm ext}\mathcal{A}$ across the sample area $\mathcal{A}$. We assume type-II superconductivity, varying the Ginzburg-Landau constant ($\kappa \in [1, \infty]$). Our companion paper [85] establishes robustness of the CV and its signature in many other systems, e.g., with different symmetries, Fermi surfaces, geometries, system sizes, additional vortices, and nonmagnetic impurities.

We use the well-established quasiclassical theory of superconductivity [86–99], solving self-consistently for the order parameter Δ and vector potential $\mathbf{A}$ [100], via the gap equation and Maxwell's equation, keeping all parameters fixed during convergence. Apart from providing attractive pair potentials in the two $d_{x^2-y^2}$- and d_{xy}-wave channels [101], and providing a chiral start guess (see below), we do not constrain the superconducting state in any way. This allows the system to choose another state, e.g., the single-component nodal d-wave state, but we always find the chiral state to be stable. We use a state-of-the-art implementation that runs on graphics processing units (GPUs) via the open-source framework SuperConga, already extensively used for studying vortex physics in conventional superconductors [99].

Chiral d-wave superconductivity. Any 2D d-wave superconducting state can be described via the order parameter $\Delta(\mathbf{p}_{\rm F}, \mathbf{R}) = \Delta_{d_{x^2-y^2}}(\mathbf{p}_{\rm F}, \mathbf{R}) + \Delta_{d_{xy}}(\mathbf{p}_{\rm F}, \mathbf{R})$. Here, $\mathbf{R}$ is the center-of-mass (c.m.) coordinate and $\mathbf{p}_{\rm F} = p_{\rm F}(\cos\theta_{\rm F}, \sin\theta_{\rm F})$ the Fermi momentum. Each component can be parametrized with amplitudes and phases as $\Delta_\Gamma(\mathbf{p}_{\rm F}, \mathbf{R}) = |\Delta_\Gamma(\mathbf{R})|e^{i\chi_\Gamma(\mathbf{R})}\eta_\Gamma(\mathbf{p}_{\rm F})$ with basis functions $\eta_{d_{x^2-y^2}}(\mathbf{p}_{\rm F}) = \sqrt{2}\cos(2\theta_{\rm F})$ and $\eta_{d_{xy}}(\mathbf{p}_{\rm F}) = \sqrt{2}\sin(2\theta_{\rm F})$. We assume degenerate nodal components, guaranteed in three- and sixfold rotational symmetric lattices [14] and thus relevant for most proposed chiral d-wave superconductors [18–31]. In Ref. [85] we establish that nondegeneracy do not change the results. A chiral d-wave state is characterized by a relative $\pi/2$ phase shift between these two d-wave components, causing TRSB [102]. To elucidate chirality, we reparametrize

$$\Delta(\mathbf{p}_{\rm F}, \mathbf{R}) = \Delta_+(\mathbf{p}_{\rm F}, \mathbf{R}) + \Delta_-(\mathbf{p}_{\rm F}, \mathbf{R}), \tag{1}$$

with $\Delta_\pm(\mathbf{p}_{\rm F}, \mathbf{R}) \equiv |\Delta_\pm(\mathbf{R})|e^{i\chi_\pm(\mathbf{R})}\eta_\pm(\mathbf{p}_{\rm F})$, where $\eta_\pm(\mathbf{p}_{\rm F}) \equiv e^{\pm i2\theta_{\rm F}}$ is the eigenbasis of the OAM operator $\hat{L}_z^{\rm orb} \equiv (\hbar/i)\partial_{\theta_{\rm F}}$, with eigenvalue $l_z^{\rm orb} = \pm 2\hbar$. Thus, the two components have opposite chirality and we refer to $\Delta_\pm$ as the chiral components, while $\Delta_{d_{x^2-y^2}}$ and $\Delta_{d_{xy}}$ are the nodal components. In a chiral superconductor, one of the two degenerate ground states, Δ_+ or Δ_-, becomes dominant just below T_c, while the other becomes subdominant. The subdominant component is fully suppressed in the bulk, but may appear at spatial inhomogeneities, such as edges, vortices, or impurities. Thus, the general form Eq. (1) is required when considering finite or vortex systems. The two chiral states $\Delta_\pm$ are fully gapped in the bulk with a nontrivial topology classified by Chern numbers ± 2 [7–14]. Hence, each state hosts two chiral edge modes traversing the bulk gap, leading to finite LDOS at boundaries at all subgap energies. Chiral d-wave superconductors can also host domain walls, which are topological defects separating regions of opposite chirality. While they generally increase the free energy, they can be stabilized, e.g., geometrically or by disorder [103]. Four chiral edge modes appear at a domain wall, two on each side and pairwise counterpropagating [104].

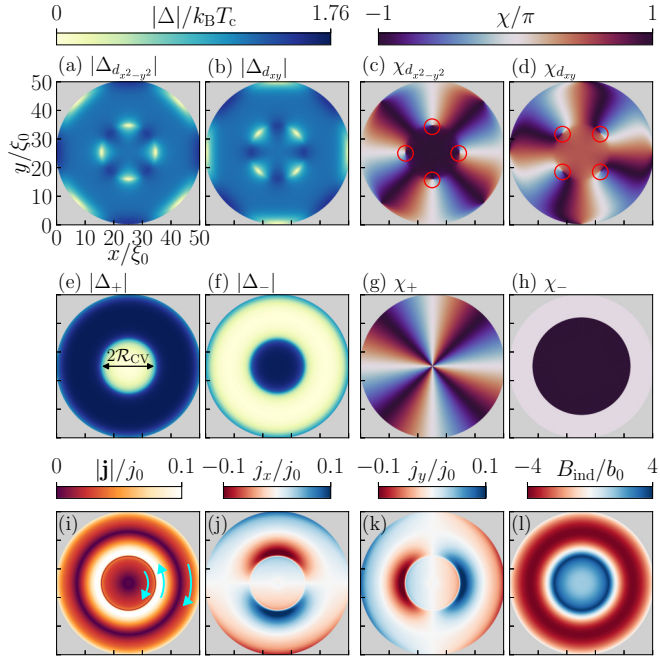

FIG. 1. CV in disk with dominant chirality Δ_+, $T = 0.1T_{\rm c}$, $\Phi_{\rm ext} = 8\Phi_0$ ($\Phi_0 \equiv hc/2|e|$), $\kappa = 80$, $\mathcal{R} = 25\xi_0$. [(a),(b)] Amplitudes and [(c),(d)] phases of the nodal components, with same in [(e)–(h)] for the chiral components. Red circles: fractional vortices. (i) Magnitude and [(j),(k)] components of the charge-current density ($j_0 \equiv 2\pi k_{\rm B}T_{\rm c}|e|N_{\rm F}v_{\rm F}$). Arrows: $\mathbf{j}$ direction. (l) Induced magnetic-flux density ($b_0 \equiv 10^{-5}\Phi_0/\pi\xi_0^2$).

Regular Abrikosov vortices are topological defects associated with a 2π phase winding that locally suppresses the order parameter into a paramagnetic and normal-state core. Superconductivity recovers over the coherence length ξ_0 from the core, with a diamagnetic screening over the penetration depth, $\lambda_0 \equiv \sqrt{c^2/(4\pi e^2 v_{\rm F}^2 N_{\rm F})}$, with the speed of light c, elementary charge $e = -|e|$, and normal-state density of states at the Fermi level $N_{\rm F}$. In a two-component order parameter, an Abrikosov vortex consists of a spatially overlapping 2π phase winding in each phase, $\chi_{d_{x^2-y^2}}$ and $\chi_{d_{xy}}$ for chiral d wave. These individual phase windings are referred to as fractional vortices, as they can carry fractional flux quantum [1,105–119]. Spatially separating them leads to a nonsingular vortex, but usually also increased energy [77], thus preventing separation. However, certain environments, especially a domain wall, can still favor separation. In fact, since a domain wall locally suppresses the order parameter, it typically attracts Abrikosov vortices, which can then split up into fractional vortices [106,120]. This is the key concept for CV formation.

Coreless vortex. Figure 1 shows a robust [121] CV computed self-consistently in a chiral d-wave superconductor. Top (middle) row shows the amplitudes and phases of the nodal (chiral) order parameter components. Of central interest is the existence of four spatially separated fractional vortices in each nodal component (red circles), showing that there are no singular vortices. The fractional vortices locally suppress the corresponding nodal amplitude and lie on a circularly formed domain wall. The domain wall is clearly seen in the

amplitudes of the chiral components as it separates an outer region with dominant chirality Δ_+ from an inner region with dominant chirality Δ_-, setting the CV radius $\mathcal{R}_{\rm CV} \approx 10\xi_0$. The dominant chiral phase χ_+ winds $-4\times 2\pi$, but the center of this winding lies in the region where already $\Delta_+ \approx 0$ (and $\Delta_- \neq 0$). The vortex is thus nonsingular and coreless. Consequently, the CV reduces the depairing caused by the external flux without paying the cost of a normal-state core, making it energetically favorable. In sharp contrast, all components are zero in Abrikosov vortex cores, see Supplemental Material (SM) [122] for comparison and generality of results vs external flux. χ_- is constant bar an irrelevant π shift, see SM [122].

We can understand the phase winding of the CV in Fig. 1 by noting that a chiral state with vorticity m has a phase winding $m \times 2\pi$ in the dominant chiral component, here with $m = -4$. Meanwhile, the subdominant chiral component is constrained to winding $p = m + 2M$ with the Chern number M set by the dominant chirality, see SM [122] for derivation. This quadruply quantized CV is the most stable CV as it corresponds to a commensurate scenario where the phase windings from the chirality and vorticity exactly cancel in the subdominant component, $p = -4 + 2 \times 2 = 0$, thus both maximizing condensation and minimizing kinetic energy. In contrast, we find that any other CV have higher energy, as $|m| \neq 4$ leads to $p \neq 0$, which both topologically suppresses Δ_- and increases the kinetic energy, see SM [122]. Hence, we find that a CV is very generally quadruply quantized in a chiral d-wave superconductor, with a total of $2|m| = 8$ fractional vortices present in the nodal components, in contrast to the double quantization found in p-wave superfluids [66].

The CV generates additional interesting properties. In Figs. 1(i)–1(l) we plot the resulting charge-current density ($\mathbf{j}$) and induced magnetic-flux density ($B_{\rm ind}$). There is a current running in opposite directions on either side of the domain wall due to its chiral edge modes. There are also chiral edge modes at the disk edges and superposed Meissner screening currents, which generates an overall nontrivial current profile. The induced flux density shows a clear paramagnetic (blue) inner region, but in contrast to an Abrikosov vortex, the maximal paramagnetism is not at the center but at the domain wall. This magnetic ring structure offers a distinct signature for scanning magnetic probes, enhanced at lower κ.

We next turn our attention to the distinct LDOS signatures of a CV. Figures 2(a)–2(d) show the LDOS $N(\varepsilon)$ subgap, developing from a single ring at the domain wall at zero energy, to two concentric ring structures emanating from the domain wall at higher energies. Figure 2(e) displays the LDOS along a line across the system and clearly shows how the ring separation grows with energy (or bias voltage). We attribute these ring-like states primarily to the vorticity, as a domain wall itself hosts only a small subgap DOS from the chiral edge modes, similar to the system edges seen in Fig. 2(e). Notably, this stands in contrast to the point-like LDOS generated in the core of an Abrikosov vortex [123–126], see SM [122].

Size and shape. The finite CV radius $\mathcal{R}_{\rm CV}$ is determined by competing forces [127]. The repulsive interaction between the fractional vortices balances an attractive surface tension from the domain wall currents, implying that the CV size is changed by anything influencing the currents or fractional

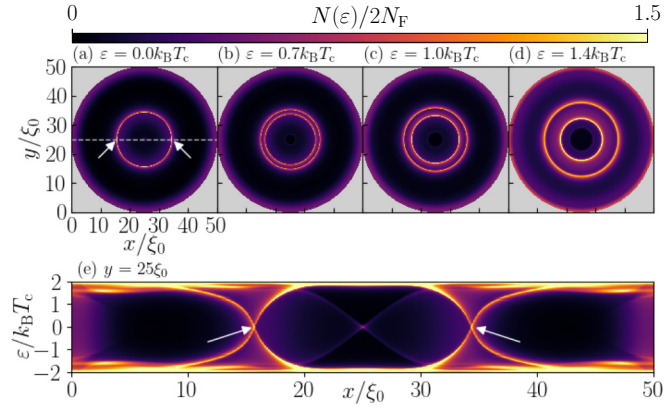

FIG. 2. CV LDOS, same parameters as Fig. 1, and broadening $\delta \approx 0.03k_{\rm B}T_{\rm c}$. [(a)–(d)] LDOS at fixed energies ε. (e) LDOS along dashed line in (a). Arrows: same points in (a) and (e).

vortices. In Figs. 3(a) and 3(b) we plot the zero-energy LDOS across a CV to show how $\mathcal{R}_{\rm CV}$ is tuned directly by both the external magnetic flux and temperature. In particular, a higher flux leads to a smaller CV due to smaller separation of the fractional vortices, in analogy with denser Abrikosov vortex lattices at higher flux. Low temperature increases both the attraction and repulsion and therefore has less of an effect, but eventually leads to a small contraction. Please note, the small peak at the disk center is only present in fully symmetrical systems. In Figs. 3(c) and 3(d) we extract the LDOS at the domain wall and illustrate how its zero-energy peak increases substantially with both external magnetic flux and temperature, even surpassing the coherence peaks and thus providing yet another clear signature of CVs. Beyond temperature and flux, we find that the penetration depth λ_0 also influences the CV, by modifying the screening currents and fractional vortex separation [85]. For $\lambda_0 > \mathcal{R}$ the CV radius $\mathcal{R}_{\rm CV}$ remains nearly constant (negligible screening), while

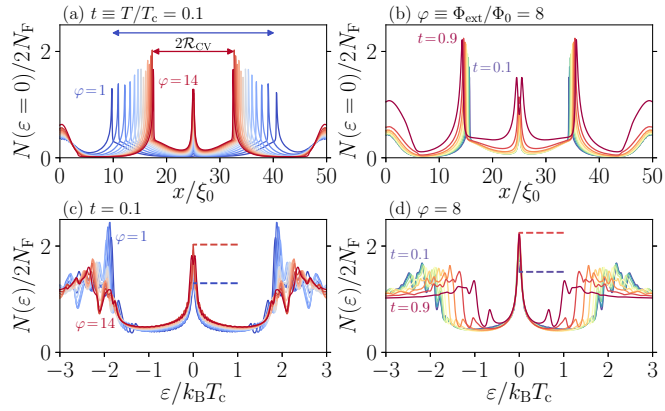

FIG. 3. [(a),(b)] Zero-energy LDOS across a CV [dashed line in Fig. 2(a)]. (a) Fixed $T = 0.1T_{\rm c}$, varying $\Phi_{\rm ext} = \Phi_0$ (blue) to $14\Phi_0$ (red). (b) Fixed $\Phi_{\rm ext} = 8\Phi_0$, varying $T = 0.1T_{\rm c}$ (blue) to $0.9T_{\rm c}$ (red). [(c),(d)] LDOS in the domain wall of a CV [arrows in Fig. 2(e)] with same parameters as (a) and (b). Horizontal arrows: CV size. Horizontal dashed lines: zero-energy peak height for high versus low flux (c), and temperature (d).

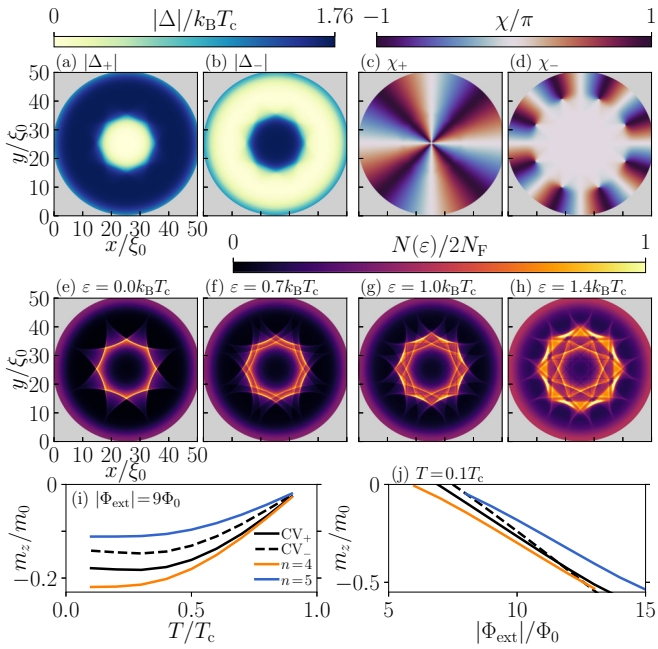

FIG. 4. CV with broken axial and rotational symmetries at $\Phi_{ext} = -8\Phi_0$, but otherwise the same parameters as Fig. 1. [(a),(b)] Chiral order parameter amplitudes and [(c),(d)] phases. [(e)–(h)] LDOS at fixed energies ε. [(i),(j)] Magnetic moment m_z for CV in positive flux (CV_+, solid lines) and $-m_z$ in negative flux (CV_-, dashed lines) or n Abrikosov vortices ($m_0 \equiv 2\mu_B N$ with Bohr magneton μ_B and particle number N [99]).

for $\lambda_0 < \mathcal{R}$, the radius shrinks monotonically to $\mathcal{R}_{CV} \approx 4\xi_0$ at $\lambda_0 = 2\xi_0$ (strong screening). Thus, adding (non)magnetic impurities should (increase) reduce $\mathcal{R}_{CV}$ [128]. Beyond radius, we find that the overall CV shape can also change in the presence of strong anisotropy caused by, e.g., the Fermi surface, geometry, or other vortices, see Ref. [85], demonstrating strong tunability, while preserving the definitive signatures established here.

Spontaneous symmetry breaking. So far, we have studied CVs in a system with dominant chirality Δ_+ for a positive external magnetic flux, $\Phi_{ext} = 8\Phi_0$. Next we show that changing to negative flux leads to inequivalent CV properties, beyond simple effects of TRSB. Specifically, antiparallel (parallel) chirality and vorticity leads to canceled (enhanced) phase winding. Note that the following negative flux results are equivalent to instead changing the dominant chirality to Δ_- [129]. Figures 4(a)–4(d) show the amplitude and phase of a CV at $\Phi_{ext} = -8\Phi_0$. We find again that the CV is quadruply quantized with winding $m = 4$ in the dominant phase χ_+. However, the subdominant χ_- has winding $p = 4 + 2 \times 2 = 8$, since the vorticity and Chern number contributions now add, rather than cancel. This asymmetry is thus not present in a TRSB but nonchiral superconductor. Furthermore, instead of an axisymmetric winding center in χ_-, there are now eight disassociated winding centers, thus spontaneously breaking axial and continuous rotational symmetries. This occurs because any axisymmetric solution would suppress Δ_- at the center thus reducing superconductivity, while here the winding centers occurs where Δ_- is already effectively zero. Importantly, these winding centers lead to additional phase gradients that deforms the domain wall into concave circular segments. The resulting CV in negative flux becomes a symmetry-broken and octagon-like solution with characteristic concave segments.

The broken symmetry is highly visible in the LDOS, see Figs. 4(e)–4(h), where the zero-energy peaks along the domain wall now takes a characteristic octagon and concave shape. More importantly, we find an even more intricate pattern at higher energies, with interweaving eight-corner concave shapes due to the eight additional winding centers, see also SM [122]. This is thus a property due to the superposed vorticity and chirality, which by definition cannot be present in a nonchiral superconductor. Taken together, LDOS measurements on a CV in opposite field directions not only discriminate chiral from nonchiral TRSB states, but also give a direct signature of the quadruple quantization, thus measuring the d-wave pairing symmetry and its Chern number. We find that these distinctive signatures survive strong broadening (see SM [122]), nondegenerate nodal components, anisotropic Fermi surfaces, irregular systems, and nonmagnetic impurities, see Ref. [85]. We attribute this broad generality to chirality and vorticity both being quantized and topological. Finally, in Figs. 4(i) and 4(j) we provide bulk signatures of CVs by showing the total orbital magnetic moment m_z [99] vs temperature and flux, clearly distinguishable for symmetric and symmetry-broken CVs, as well as from Abrikosov vortices. Since experiments can already distinguish the spectroscopic and magnetic signatures from different number of Abrikosov vortices [130], Figs. 4(i) and 4(j) show that they should also be able to distinguish the symmetric and symmetry-broken CVs. Furthermore, the overall offset and slope varies between different vortex solutions, tunable by fixing temperature or flux, while measuring as a function of the other.

To summarize, we establish quadruply quantized CVs as smoking-gun signatures of chiral d-wave superconductivity. These CVs are stable and consist of a closed domain wall with eight isolated fractional vortices, with a radius tunable by external flux, temperature, and material properties. While the CV is circular symmetric in one field direction, it spontaneously breaks rotational and axial symmetries in the other, together resulting in direct fingerprints of TRSB, chiral superconductivity, d-wave symmetry, and the Chern number, in both the LDOS and magnetic moment. Applying our results to earlier study [66], we conclude that a square-shaped CV LDOS in a chiral p wave may likewise be a signature of both p-wave pairing symmetry and $M = \pm 1$ Chern number. Beyond these direct experimental signatures, our results also establish chiral d-wave superconductors as platforms for realizing fractional vortices and chiral $\mathbb{C}P^1$ skyrmions [76–79,131,132], highly relevant in both magnetic materials and liquid crystals [133,134] as well as in particle and high-energy physics [135–138].

Note added. A preprint [139] appeared about skyrmionic chains in a twisted-bilayer model using Ginzburg-Landau theory. Using a pseudospin formalism [131], the CVs in our paper are analogous to chiral $\mathbb{C}P^1$ skyrmions [79] here with skyrmion number $Q = 4$, which are different from the skyrmionic chains. Moreover, we establish the experimental

accessible signatures for distinguishing time-reversal symmetry breaking, chiral superconductivity, and the Chern number.

Acknowledgments. We thank M. Fogelström and A. B. Vorontsov for valuable discussions, and N. Wall-Wennerdal, T. Löfwander, M. Håkansson, O. Shevtsov, P. Stadler, and M. Fogelström for their work on SuperConga. We acknowledge financial support from the European Research Council (ERC) under the European Union Horizon 2020 research and innovation programme (Grant No. ERC-2017-StG-757553) and the Knut and Alice Wallenberg Foundation through the Wallenberg Academy Fellows program. The computations were enabled by the supercomputing resource Berzelius provided by National Supercomputer Centre (NSC) at Linköping University and the Knut and Alice Wallenberg Foundation. Additional computations were enabled by resources provided by the National Academic Infrastructure for Supercomputing in Sweden (NAISS) and the Swedish National Infrastructure for Computing (SNIC) at C3SE, HPC2N, and NSC, partially funded by the Swedish Research Council through Grant Agreements No. 2022-06725 and No. 2018-05973.

[1] M. Sigrist and K. Ueda, Phenomenological theory of unconventional superconductivity, Rev. Mod. Phys. **63**, 239 (1991).

[2] G. Volovik, *The Universe in a Helium Droplet* (Oxford University Press, Oxford, 2003).

[3] C. Kallin and J. Berlinsky, Chiral superconductors, Rep. Prog. Phys. **79**, 054502 (2016).

[4] T. Mizushima, Y. Tsutsumi, T. Kawakami, M. Sato, M. Ichioka, and K. Machida, Symmetry-protected topological superfluids and superconductors—From the basics to ^{3}He, J. Phys. Soc. Jpn. **85**, 022001 (2016).

[5] G. E. Volovik, Topological superfluids, J. Exp. Theor. Phys. **129**, 618 (2019).

[6] G. E. Volovik, ^{3}He Universe 2020, J. Low Temp. Phys. **202**, 11 (2021).

[7] G. E. Volovik, On edge states in superconductors with time inversion symmetry breaking, JETP Lett. **66**, 522 (1997).

[8] A. P. Schnyder, S. Ryu, A. Furusaki, and A. W. W. Ludwig, Classification of topological insulators and superconductors in three spatial dimensions, Phys. Rev. B **78**, 195125 (2008).

[9] M. Z. Hasan and C. L. Kane, Colloquium: Topological insulators, Rev. Mod. Phys. **82**, 3045 (2010).

[10] X.-L. Qi and S.-C. Zhang, Topological insulators and superconductors, Rev. Mod. Phys. **83**, 1057 (2011).

[11] J. A. Sauls, Surface states, edge currents, and the angular momentum of chiral *p*-wave superfluids, Phys. Rev. B **84**, 214509 (2011).

[12] Y. Tanaka, M. Sato, and N. Nagaosa, Symmetry and topology in superconductors 'odd-frequency pairing and edge states', J. Phys. Soc. Jpn. **81**, 011013 (2012).

[13] G. M. Graf and M. Porta, Bulk-edge correspondence for two-dimensional topological insulators, Commun. Math. Phys. **324**, 851 (2013).

[14] A. M. Black-Schaffer and C. Honerkamp, Chirald-wave superconductivity in doped graphene, J. Phys.: Condens. Matter **26**, 423201 (2014).

[15] C. Kallin, Chiral p-wave order in Sr_2RuO_4, Rep. Prog. Phys. **75**, 042501 (2012).

[16] O. Can, T. Tummuru, R. P. Day, I. Elfimov, A. Damascelli, and M. Franz, High-temperature topological superconductivity in twisted double-layer copper oxides, Nat. Phys. **17**, 519 (2021).

[17] O. Can, X.-X. Zhang, C. Kallin, and M. Franz, Probing Time Reversal Symmetry Breaking Topological Superconductivity in Twisted Double Layer Copper Oxides with Polar Kerr Effect, Phys. Rev. Lett. **127**, 157001 (2021).

[18] J. W. F. Venderbos and R. M. Fernandes, Correlations and electronic order in a two-orbital honeycomb lattice model for twisted bilayer graphene, Phys. Rev. B **98**, 245103 (2018).

[19] Y. Su and S.-Z. Lin, Pairing symmetry and spontaneous vortex-antivortex lattice in superconducting twisted-bilayer graphene: Bogoliubov-de Gennes approach, Phys. Rev. B **98**, 195101 (2018).

[20] M. Fidrysiak, M. Zegrodnik, and J. Spałek, Unconventional topological superconductivity and phase diagram for an effective two-orbital model as applied to twisted bilayer graphene, Phys. Rev. B **98**, 085436 (2018).

[21] C. Xu and L. Balents, Topological Superconductivity in Twisted Multilayer Graphene, Phys. Rev. Lett. **121**, 087001 (2018).

[22] D. M. Kennes, J. Lischner, and C. Karrasch, Strong correlations and $d + id$ superconductivity in twisted bilayer graphene, Phys. Rev. B **98**, 241407(R) (2018).

[23] C.-C. Liu, L.-D. Zhang, W.-Q. Chen, and F. Yang, Chiral Spin Density Wave and $d + id$ Superconductivity in the Magic-Angle-Twisted Bilayer Graphene, Phys. Rev. Lett. **121**, 217001 (2018).

[24] H. Guo, X. Zhu, S. Feng, and R. T. Scalettar, Pairing symmetry of interacting fermions on a twisted bilayer graphene superlattice, Phys. Rev. B **97**, 235453 (2018).

[25] F. Wu, Topological chiral superconductivity with spontaneous vortices and supercurrent in twisted bilayer graphene, Phys. Rev. B **99**, 195114 (2019).

[26] A. Fischer, L. Klebl, C. Honerkamp, and D. M. Kennes, Spin-fluctuation-induced pairing in twisted bilayer graphene, Phys. Rev. B **103**, L041103 (2021).

[27] F. Ming, X. Wu, C. Chen, K. D. Wang, P. Mai, T. A. Maier, J. Strockoz, J. W. F. Venderbos, C. González, J. Ortega, S. Johnston, and H. H. Weitering, Evidence for chiral superconductivity on a silicon surface, Nat. Phys. **19**, 500 (2023).

[28] P. K. Biswas, H. Luetkens, T. Neupert, T. Stürzer, C. Baines, G. Pascua, A. P. Schnyder, M. H. Fischer, J. Goryo, M. R. Lees, H. Maeter, F. Brückner, H.-H. Klauss, M. Nicklas, P. J. Baker, A. D. Hillier, M. Sigrist, A. Amato, and D. Johrendt, Evidence for superconductivity with broken time-reversal symmetry in locally noncentrosymmetric srptas, Phys. Rev. B **87**, 180503(R) (2013).

[29] M. H. Fischer, T. Neupert, C. Platt, A. P. Schnyder, W. Hanke, J. Goryo, R. Thomale, and M. Sigrist, Chiral *d*-wave superconductivity in SrPtAs, Phys. Rev. B **89**, 020509(R) (2014).

[30] H. Ueki, R. Tamura, and J. Goryo, Possibility of chiral *d*-wave state in the hexagonal pnictide superconductor SrPtAs, Phys. Rev. B **99**, 144510 (2019).

[31] H. Ueki, S. Inagaki, R. Tamura, J. Goryo, Y. Imai, W. B. Rui, A. P. Schnyder, and M. Sigrist, Phenomenology of the chiral

d-wave state in the hexagonal pnictide superconductor SrPtAs, JPS Conf. Proc. **30**, 011044 (2020).

[32] P. K. Biswas, S. K. Ghosh, J. Z. Zhao, D. A. Mayoh, N. D. Zhigadlo, X. Xu, C. Baines, A. D. Hillier, G. Balakrishnan, and M. R. Lees, Chiral singlet superconductivity in the weakly correlated metal $LaPt_3P$, Nat. Commun. **12**, 2504 (2021).

[33] X. Gong, M. Kargarian, A. Stern, D. Yue, H. Zhou, X. Jin, V. M. Galitski, V. M. Yakovenko, and J. Xia, Time-reversal symmetry-breaking superconductivity in epitaxial bismuth/nickel bilayers, Sci. Adv. **3**, e1602579 (2017).

[34] H. Hosseinabadi and M. Kargarian, Vortex bound states of charge and magnetic fluctuations induced topological superconductors in heterostructures, Phys. Rev. B **100**, 144507 (2019).

[35] Y. Kasahara, T. Iwasawa, H. Shishido, T. Shibauchi, K. Behnia, Y. Haga, T. D. Matsuda, Y. Onuki, M. Sigrist, and Y. Matsuda, Exotic Superconducting Properties in the Electron-Hole-Compensated Heavy-Fermion "Semimetal" URu_2Si_2, Phys. Rev. Lett. **99**, 116402 (2007).

[36] Y. Kasahara, H. Shishido, T. Shibauchi, Y. Haga, T. D. Matsuda, Y. Onuki, and Y. Matsuda, Superconducting gap structure of heavy-fermion compound URu_2Si_2 determined by angle-resolved thermal conductivity, New J. Phys. **11**, 055061 (2009).

[37] T. Shibauchi, H. Ikeda, and Y. Matsuda, Broken symmetries in URu_2Si_2, Philos. Mag. **94**, 3747 (2014).

[38] Y. Iguchi, I. P. Zhang, E. D. Bauer, F. Ronning, J. R. Kirtley, and K. A. Moler, Local observation of linear-*t* superfluid density and anomalous vortex dynamics in URu_2Si_2, Phys. Rev. B **103**, L220503 (2021).

[39] A. Mercado, S. Sahoo, and M. Franz, High-Temperature Majorana Zero Modes, Phys. Rev. Lett. **128**, 137002 (2022).

[40] G. Margalit, B. Yan, M. Franz, and Y. Oreg, Chiral Majorana modes via proximity to a twisted cuprate bilayer, Phys. Rev. B **106**, 205424 (2022).

[41] Y. Huang, S.-S. Gong, and D. N. Sheng, Quantum Phase Diagram and Spontaneously Emergent Topological Chiral Superconductivity in Doped Triangular-Lattice Mott Insulators, Phys. Rev. Lett. **130**, 136003 (2023).

[42] W. Huang, E. Taylor, and C. Kallin, Vanishing edge currents in non-*p*-wave topological chiral superconductors, Phys. Rev. B **90**, 224519 (2014).

[43] Y. Tada, W. Nie, and M. Oshikawa, Orbital Angular Momentum and Spectral Flow in Two-Dimensional Chiral Superfluids, Phys. Rev. Lett. **114**, 195301 (2015).

[44] G. E. Volovik, Orbital momentum of chiral superfluids and the spectral asymmetry of edge states, JETP Lett. **100**, 742 (2015).

[45] S.-I. Suzuki and Y. Asano, Spontaneous edge current in a small chiral superconductor with a rough surface, Phys. Rev. B **94**, 155302 (2016).

[46] X. Wang, Z. Wang, and C. Kallin, Spontaneous edge current in higher chirality superconductors, Phys. Rev. B **98**, 094501 (2018).

[47] W. Nie, W. Huang, and H. Yao, Edge current and orbital angular momentum of chiral superfluids revisited, Phys. Rev. B **102**, 054502 (2020).

[48] E. Sugiyama and S. Higashitani, Surface bound states and spontaneous edge currents in chiral superconductors: Effect of spatially varying order parameter, J. Phys. Soc. Jpn. **89**, 034706 (2020).

[49] P. Holmvall and A. M. Black-Schaffer, Enhanced chiral edge currents and orbital magnetic moment in chiral *d*-wave superconductors from mesoscopic finite-size effects, arXiv:2308.15258.

[50] G. E. Volovik, An analog of the quantum Hall effect in a superfluid ^{3}He film, JETP Lett. **67**, 1804 (1988).

[51] A. M. Black-Schaffer, Edge Properties and Majorana Fermions in the Proposed Chiral *d*-Wave Superconducting State of Doped Graphene, Phys. Rev. Lett. **109**, 197001 (2012).

[52] N. D. Mermin and T.-L. Ho, Circulation and Angular Momentum in the *a* Phase of Superfluid Helium-3, Phys. Rev. Lett. **36**, 594 (1976).

[53] P. W. Anderson and G. Toulouse, Phase Slippage without Vortex Cores: Vortex Textures in Superfluid ^{3}He, Phys. Rev. Lett. **38**, 508 (1977).

[54] T.-L. Ho, Coreless vortices in superfluid ^{3}He-*a*: Topological structure, nucleation, and the screening effect, Phys. Rev. B **18**, 1144 (1978).

[55] M. M. Salomaa and G. E. Volovik, Quantized vortices in superfluid ^{3}He, Rev. Mod. Phys. **59**, 533 (1987).

[56] R. Rantanen and V. B. Eltsov, Transition in vortex skyrmion structures in superfluid ^{3}He$-a$ driven by an analog of the zero-charge effect, Phys. Rev. B **107**, 104505 (2023).

[57] P. J. Hakonen, O. T. Ikkala, and S. T. Islander, Experiments on Vortices in Rotating Superfluid ^{3}He-*A*, Phys. Rev. Lett. **49**, 1258 (1982).

[58] H. K. Seppälä and G. E. Volovik, Evidence for nonsingular vorticity in the Helsinki experiments on rotating ^{3}He-*A*, J. Low Temp. Phys. **51**, 279 (1983).

[59] H. K. Seppälä, P. J. Hakonen, M. Krusius, T. Ohmi, M. M. Salomaa, J. T. Simola, and G. E. Volovik, Continuous Vortices with Broken Symmetry in Rotating Superfluid ^{3}He-*A*, Phys. Rev. Lett. **52**, 1802 (1984).

[60] E. V. Thuneberg, Identification of Vortices in Superfluid ^3B, Phys. Rev. Lett. **56**, 359 (1986).

[61] U. Parts, J. M. Karimäki, J. H. Koivuniemi, M. Krusius, V. M. H. Ruutu, E. V. Thuneberg, and G. E. Volovik, Phase Diagram of Vortices in Superfluid ^{3}He-*A*, Phys. Rev. Lett. **75**, 3320 (1995).

[62] V. M. H. Ruutu, J. Kopu, M. Krusius, U. Parts, B. Plaçais, E. V. Thuneberg, and W. Xu, Critical Velocity of Vortex Nucleation in Rotating Superfluid ^{3}He-*A*, Phys. Rev. Lett. **79**, 5058 (1997).

[63] O. V. Lounasmaa and E. Thuneberg, Vortices in rotating superfluid ^{3}He, Proc. Natl. Acad. Sci. USA **96**, 7760 (1999).

[64] R. Blaauwgeers, V. B. Eltsov, M. Krusius, J. J. Ruohio, R. Schanen, and G. E. Volovik, Double-quantum vortex in superfluid ^{3}He-*A*, Nature (London) **404**, 471 (2000).

[65] P. M. Walmsley, D. J. Cousins, and A. I. Golov, Critical Velocity of Continuous Vortex Nucleation in a Slab of Superfluid ^{3}He-*A*, Phys. Rev. Lett. **91**, 225301 (2003).

[66] J. A. Sauls and M. Eschrig, Vortices in chiral, spin-triplet superconductors and superfluids, New J. Phys. **11**, 075008 (2009).

[67] J. Garaud and E. Babaev, Skyrmionic state and stable half-quantum vortices in chiral *p*-wave superconductors, Phys. Rev. B **86**, 060514(R) (2012).

[68] J. Garaud and E. Babaev, Properties of skyrmions and multi-quanta vortices in chiral p-wave superconductors, Sci. Rep. **5**, 17540 (2015).

[69] J. Garaud, E. Babaev, T. A. Bojesen, and A. Sudbø, Lattices of double-quanta vortices and chirality inversion in $p_x + ip_y$ superconductors, Phys. Rev. B **94**, 104509 (2016).

[70] L.-F. Zhang, V. F. Becerra, L. Covaci, and M. V. Milošević, Electronic properties of emergent topological defects in chiral p-wave superconductivity, Phys. Rev. B **94**, 024520 (2016).

[71] V. Fernández Becerra, E. Sardella, F. M. Peeters, and M. V. Milošević, Vortical versus skyrmionic states in mesoscopic p-wave superconductors, Phys. Rev. B **93**, 014518 (2016).

[72] A. A. Zyuzin, J. Garaud, and E. Babaev, Nematic Skyrmions in Odd-Parity Superconductors, Phys. Rev. Lett. **119**, 167001 (2017).

[73] G.-Q. Zha, Vortical configurations in mesoscopic superconducting square loop with mixed pairing orders, Europhys. Lett. **130**, 67005 (2020).

[74] R.-F. Chai and G.-Q. Zha, Vortical patterns in bulk superconducting systems with mixed pairing orders, Eur. Phys. J. B **94**, 98 (2021).

[75] F. N. Krohg, E. Babaev, J. Garaud, H. H. Haugen, and A. Sudbø, Thermal fluctuations and vortex lattice structures in chiral p-wave superconductors: Robustness of double-quanta vortices, Phys. Rev. B **103**, 214517 (2021).

[76] J. Garaud, J. Carlström, and E. Babaev, Topological Solitons in Three-Band Superconductors with Broken Time Reversal Symmetry, Phys. Rev. Lett. **107**, 197001 (2011).

[77] J. Garaud, J. Carlström, E. Babaev, and M. Speight, Chiral $\mathbb{C}P^2$ skyrmions in three-band superconductors, Phys. Rev. B **87**, 014507 (2013).

[78] T. Winyard, M. Silaev, and E. Babaev, Skyrmion formation due to unconventional magnetic modes in anisotropic multiband superconductors, Phys. Rev. B **99**, 024501 (2019).

[79] A. Benfenati, M. Barkman, and E. Babaev, Demonstration of $\mathbb{C}P^2$ skyrmions in three-band superconductors by self-consistent solutions of a Bogoliubov–de Gennes model, Phys. Rev. B **107**, 094503 (2023).

[80] A. M. Black-Schaffer and S. Doniach, Resonating valence bonds and mean-field d-wave superconductivity in graphite, Phys. Rev. B **75**, 134512 (2007).

[81] K. Takada, H. Sakurai, E. Takayama-Muromachi, F. Izumi, R. A. Dilanian, and T. Sasaki, Superconductivity in two-dimensional CoO_2 layers, Nature (London) **422**, 53 (2003).

[82] M. L. Kiesel, C. Platt, W. Hanke, and R. Thomale, Model Evidence of an Anisotropic Chiral $d+id$-Wave Pairing State for the Water-Intercalated $Na_xCoO_2 \cdot yH_2O$ Superconductor, Phys. Rev. Lett. **111**, 097001 (2013).

[83] S. Yamanaka, K.-i. Hotehama, and H. Kawaji, Superconductivity at 25.5 k in electron-doped layered hafnium nitride, Nature (London) **392**, 580 (1998).

[84] K. Kuroki, Spin-fluctuation-mediated $d + id'$ pairing mechanism in doped $\beta-m\mathrm{NCl}(m = \mathrm{Hf}, \mathrm{Zr})$ superconductors, Phys. Rev. B **81**, 104502 (2010).

[85] P. Holmvall, N. Wall-Wennerdal, and A. M. Black-Schaffer, companion paper, Robust and tunable coreless vortices and fractional vortices in chiral d-wave superconductors, Phys. Rev. B **108**, 094511 (2023).

[86] G. Eilenberger, Transformation of Gorkov's equation for type II superconductors into transport-like equations, Z. Phys. **214**, 195 (1968).

[87] A. I. Larkin and Y. N. Ovchinnikov, Quasiclassical method in the theory of superconductivity, Zh. Eksp. Teor. Fiz. **55**, 2262 (1969).

[88] J. Serene and D. Rainer, The quasiclassical approach to superfluid ^{3}He, Phys. Rep. **101**, 221 (1983).

[89] A. L. Shelankov, On the derivation of quasiclassical equations for superconductors, J. Low Temp. Phys. **60**, 29 (1985).

[90] Y. Nagato, K. Nagai, and J. Hara, Theory of the Andreev reflection and the density of states in proximity contact normal-superconducting infinite double-layer, J. Low Temp. Phys. **93**, 33 (1993).

[91] M. Eschrig, J. Heym, and D. Rainer, Corrections to Fermi-liquid theory of correlated metals, J. Low Temp. Phys. **95**, 323 (1994).

[92] N. Schopohl and K. Maki, Quasiparticle spectrum around a vortex line in a d-wave superconductor, Phys. Rev. B **52**, 490 (1995).

[93] N. Schopohl, Transformation of the Eilenberger equations of superconductivity to a scalar Riccati equation, arXiv:cond-mat/9804064v1.

[94] M. Eschrig, D. Rainer, and J. A. Sauls, Effects of strong magnetic fields on pairing fluctuations in high-temperature superconductors, Phys. Rev. B **59**, 12095 (1999).

[95] M. Eschrig, Distribution functions in nonequilibrium theory of superconductivity and Andreev spectroscopy in unconventional superconductors, Phys. Rev. B **61**, 9061 (2000).

[96] M. Eschrig, Scattering problem in nonequilibrium quasiclassical theory of metals and superconductors: General boundary conditions and applications, Phys. Rev. B **80**, 134511 (2009).

[97] R. Grein, T. Löfwander, and M. Eschrig, Inverse proximity effect and influence of disorder on triplet supercurrents in strongly spin-polarized ferromagnets, Phys. Rev. B **88**, 054502 (2013).

[98] K. M. Seja and T. Löfwander, Finite element method for the quasiclassical theory of superconductivity, Phys. Rev. B **106**, 144511 (2022).

[99] P. Holmvall, N. Wall-Wennerdal, M. Håkansson, P. Stadler, O. Shevtsov, T. Löfwander, and M. Fogelström, Superconga: An open-source framework for mesoscopic superconductivity, Appl. Phys. Rev. **10**, 011317 (2023).

[100] Our self-consistency criterion is a relative error $< 10^{-7}$ for Δ, $\mathbf{A}$, $\mathbf{j}$, free energy Ω, and boundary condition.

[101] Other subdominant pair correlations compatible within group theory, e.g., s wave, are also included [99].

[102] M. Sigrist, Time-reversal symmetry breaking states in high-temperature superconductors, Prog. Theor. Phys. **99**, 899 (1998).

[103] J. Garaud and E. Babaev, Domain Walls and Their Experimental Signatures in $s + is$ Superconductors, Phys. Rev. Lett. **112**, 017003 (2014).

[104] O. A. Awoga, A. Bouhon, and A. M. Black-Schaffer, Domain walls in a chiral d-wave superconductor on the honeycomb lattice, Phys. Rev. B **96**, 014521 (2017).

[105] G. Volovik and V. Mineev, Line and point singularities in superfluid He3, Sov. Phys. JETP **24**, 561 (1976).

[106] M. Sigrist, T. M. Rice, and K. Ueda, Low-Field Magnetic Response of Complex Superconductors, Phys. Rev. Lett. **63**, 1727 (1989).
[107] G. E. Volovik, Monopoles and fractional vortices in chiral superconductors, Proc. Natl. Acad. Sci. USA **97**, 2431 (2000).
[108] C. C. Tsuei and J. R. Kirtley, Pairing symmetry in cuprate superconductors, Rev. Mod. Phys. **72**, 969 (2000).
[109] C. Tsuei and J. Kirtley, d-wave pairing symmetry in cuprate superconductors, Physica C: Superconductivity **341-348**, 1625 (2000).
[110] E. Babaev, Vortices with Fractional Flux in Two-Gap Superconductors and in Extended Faddeev Model, Phys. Rev. Lett. **89**, 067001 (2002).
[111] E. Babaev, Vortices carrying an arbitrary fraction of magnetic flux quantum, neutral superfluidity and knotted solitons in two-gap Ginzburg-Landau model, Physica C: Superconductivity **404**, 39 (2004).
[112] E. Babaev and N. W. Ashcroft, Violation of the London law and Onsager-Feynman quantization in multicomponent superconductors, Nat. Phys. **3**, 530 (2007).
[113] L. F. Chibotaru, V. H. Dao, and A. Ceulemans, Thermodynamically stable noncomposite vortices in mesoscopic two-gap superconductors, Europhys. Lett. **78**, 47001 (2007).
[114] L. F. Chibotaru and V. H. Dao, Stable fractional flux vortices in mesoscopic superconductors, Phys. Rev. B **81**, 020502(R) (2010).
[115] M. A. Silaev, Stable fractional flux vortices and unconventional magnetic state in two-component superconductors, Phys. Rev. B **83**, 144519 (2011).
[116] J. C. Piña, C. C. de Souza Silva, and M. V. Milošević, Stability of fractional vortex states in a two-band mesoscopic superconductor, Phys. Rev. B **86**, 024512 (2012).
[117] V. P. Mineev, Half-quantum vortices, Low Temp. Phys. **39**, 818 (2013).
[118] S. Autti, V. V. Dmitriev, J. T. Mäkinen, A. A. Soldatov, G. E. Volovik, A. N. Yudin, V. V. Zavjalov, and V. B. Eltsov, Observation of Half-Quantum Vortices in Topological Superfluid ^{3}He, Phys. Rev. Lett. **117**, 255301 (2016).
[119] Y. Iguchi, R. A. Shi, K. Kihou, C.-H. Lee, M. Barkman, A. L. Benfenati, V. Grinenko, E. Babaev, and K. A. Moler, Superconducting vortices carrying a temperature-dependent fraction of the flux quantum, Science **380**, 1244 (2023).
[120] M. Sigrist and D. F. Agterberg, The Role of Domain Walls on the Vortex Creep Dynamics in Unconventional Superconductors, Prog. Theor. Phys. **102**, 965 (1999).
[121] CVs are extremely robust even when metastable, and appear spontaneously instead of Abrikosov vortices for many Φ and T. Close to $B_{c,2}(T)$ the CV can become the ground state, similar to chiral p-wave superfluids [69,75,140]. A full Φ-T phase diagram is left as outlook.
[122] See Supplemental Material at http://link.aps.org/supplemental/10.1103/PhysRevB.108.L100506 for further details. In summary, Section S-1 illustrates clear differences between a CV and a regular Abrikosov vortex. Section S-2 studies phase shifts across the CV domain wall. Section S-3 derives the phase winding constraints in the chiral order parameter components. Section S-4 includes additional plots for symmetry-broken CVs. Section S-5 demonstrates that the main results and experimental signatures are robust in the presence of strong energy broadening effects. The material includes Refs. [42,47,66,85,86,99,108,123–126,141–169].
[123] C. Caroli, P. De Gennes, and J. Matricon, Bound fermion states on a vortex line in a type II superconductor, Phys. Lett. **9**, 307 (1964).
[124] D. Rainer, J. A. Sauls, and D. Waxman, Current carried by bound states of a superconducting vortex, Phys. Rev. B **54**, 10094 (1996).
[125] C. Berthod, I. Maggio-Aprile, J. Bruér, A. Erb, and C. Renner, Observation of Caroli–de Gennes–Matricon Vortex States in $YBa_2Cu_3O_{7-\delta}$, Phys. Rev. Lett. **119**, 237001 (2017).
[126] H. Kim, Y. Nagai, L. Rózsa, D. Schreyer, and R. Wiesendanger, Anisotropic non-split zero-energy vortex bound states in a conventional superconductor, Appl. Phys. Rev. **8**, 031417 (2021).
[127] G. E. Volovik, Superfluids in rotation: Landau-Lifshitz vortex sheets vs Onsager-Feynman vortices, Phys. Usp. **58**, 897 (2015).
[128] R. Prozorov, M. Zarea, and J. A. Sauls, Niobium in the clean limit: An intrinsic type-I superconductor, Phys. Rev. B **106**, L180505 (2022).
[129] Results are related via the time-reversal operation $\mathcal{T}\{\boldsymbol{B}_{\rm ext}, \Delta_\pm\} \to \{-\boldsymbol{B}_{\rm ext}, \Delta_\mp^*\}$ [67]. Hence, results for one chirality in both field directions can be mapped to results for both chiralities in one field direction.
[130] M. Timmermans, L. Serrier-Garcia, M. Perini, J. Van de Vondel, and V. V. Moshchalkov, Direct observation of condensate and vortex confinement in nanostructured superconductors, Phys. Rev. B **93**, 054514 (2016).
[131] E. Babaev, L. D. Faddeev, and A. J. Niemi, Hidden symmetry and knot solitons in a charged two-condensate Bose system, Phys. Rev. B **65**, 100512(R) (2002).
[132] L.-F. Zhang, Y.-Y. Zhang, G.-Q. Zha, M. V. Milošević, and S.-P. Zhou, Skyrmionic chains and lattices in $s + id$ superconductors, Phys. Rev. B **101**, 064501 (2020).
[133] N. Nagaosa and Y. Tokura, Topological properties and dynamics of magnetic skyrmions, Nat. Nanotechnol. **8**, 899 (2013).
[134] D. Foster, C. Kind, P. J. Ackerman, J.-S. B. Tai, M. R. Dennis, and I. I. Smalyukh, Two-dimensional skyrmion bags in liquid crystals and ferromagnets, Nat. Phys. **15**, 655 (2019).
[135] T. Skyrme, A unified field theory of mesons and baryons, Nucl. Phys. **31**, 556 (1962).
[136] N. Manton and P. Sutcliffe, *Topological Solitons*, Cambridge Monographs on Mathematical Physics (Cambridge University Press, Cambridge, 2004).
[137] Y. Akagi, Y. Amari, S. B. Gudnason, M. Nitta, and Y. Shnir, Fractional skyrmion molecules in a $\mathbb{C}$PN-1 model, J. High Energy Phys. 11 (2021) 194.
[138] H. Zhang, Z. Wang, D. Dahlbom, K. Barros, and C. D. Batista, CP^2 skyrmions and skyrmion crystals in realistic quantum magnets, Nat. Commun. **14**, 3626 (2022).
[139] L. R. Cadorim, E. Sardella, and M. V. Milošević, Vortical versus skyrmionic states in the topological phase of a twisted bilayer with d-wave superconducting pairing, arXiv:2206.14937.
[140] T. Tokuyasu and J. Sauls, Stability of doubly quantized vortices in unconventional superconductors, Phys. B: Condens. Matter **165-166**, 347 (1990).
[141] H. F. Hess, R. B. Robinson, R. C. Dynes, J. M. Valles, and

J. V. Waszczak, Scanning-Tunneling-Microscope Observation of the Abrikosov Flux Lattice and the Density of States near and inside a Fluxoid, Phys. Rev. Lett. **62**, 214 (1989).

[142] R. Heeb and D. F. Agterberg, Ginzburg-Landau theory for a *p*-wave Sr_2RuO_4 superconductor: Vortex core structure and extended london theory, Phys. Rev. B **59**, 7076 (1999).

[143] C. Renner, A. D. Kent, P. Niedermann, Ø. Fischer, and F. Lévy, Scanning Tunneling Spectroscopy of a Vortex Core from the Clean to the Dirty Limit, Phys. Rev. Lett. **67**, 1650 (1991).

[144] S. Yip and A. Garg, Superconducting states of reduced symmetry: General order parameters and physical implications, Phys. Rev. B **48**, 3304 (1993).

[145] J. A. Sauls, A theory for the superconducting phases of UPt3, J. Low Temp. Phys. **95**, 153 (1994).

[146] I. Maggio-Aprile, C. Renner, A. Erb, E. Walker, and O. Fischer, Direct Vortex Lattice Imaging and Tunneling Spectroscopy of Flux Lines on $YBa_2Cu_3O_{7-\delta}$, Phys. Rev. Lett. **75**, 2754 (1995).

[147] A. K. Geim, I. V. Grigorieva, S. V. Dubonos, J. G. S. Lok, J. C. Maan, A. E. Filippov, and F. M. Peeters, Phase transitions in individual sub-micrometre superconductors, Nature (London) **390**, 259 (1997).

[148] A. Yazdani, B. Jones, C. Lutz, M. F. Crommie, and D. M. Eigler, Probing the local effects of magnetic impurities on superconductivity, Science **275**, 1767 (1997).

[149] A. Poenicke, Y. S. Barash, C. Bruder, and V. Istyukov, Broadening of Andreev bound states in $d_{x^2-y^2}$ superconductors, Phys. Rev. B **59**, 7102 (1999).

[150] S. H. Pan, E. W. Hudson, A. K. Gupta, K.-W. Ng, H. Eisaki, S. Uchida, and J. C. Davis, STM Studies of the Electronic Structure of Vortex Cores in $Bi_2Sr_2CaCu_2O_{8+\delta}$, Phys. Rev. Lett. **85**, 1536 (2000).

[151] S. Pan, E. Hudson, K. Lang, H. Eisaki, S. Uchida, and J. Davis, Imaging the effects of individual zinc impurity atoms on superconductivity in $Bi_2Sr_2CaCu_2O_{8+\delta}$, Nature (London) **403**, 746 (2000).

[152] T. Löfwander, V. S. Shumeiko, and G. Wendin, Andreev bound states in high-*Tc* superconducting junctions, Supercond. Sci. Technol. **14**, R53 (2001).

[153] M. Ichioka and K. Machida, Field dependence of the vortex structure in chiral p-wave superconductors, Phys. Rev. B **65**, 224517 (2002).

[154] J. E. Hoffman, E. W. Hudson, K. M. Lang, V. Madhavan, H. Eisaki, S. Uchida, and J. C. Davis, A four unit cell periodic pattern of quasi-particle states surrounding vortex cores in $Bi_2Sr_2CaCu_2O_{8+\delta}$, Science **295**, 466 (2002).

[155] M. Morelle, J. Bekaert, and V. V. Moshchalkov, Influence of sample geometry on vortex matter in superconducting microstructures, Phys. Rev. B **70**, 094503 (2004).

[156] J. R. Kirtley, C. Tsuei, C. Ariando, S. Harkema, and H. Hilgenkamp, Angle-resolved phase-sensitive determination of the in-plane gap symmetry in YBa_2Cu_3O7-δ, Nat. Phys. **2**, 190 (2006).

[157] I. Guillamòn, H. Suderow, S. Vieira, L. Cario, P. Diener, and P. Rodière, Superconducting Density of States and Vortex Cores of 2H-NbS_2, Phys. Rev. Lett. **101**, 166407 (2008).

[158] V. V. Khotkevych, M. V. Milošević, and S. J. Bending, A scanning Hall probe microscope for high resolution magnetic imaging down to 300 mk, Rev. Sci. Instrum. **79**, 123708 (2008).

[159] N. Kokubo, S. Okayasu, A. Kanda, and B. Shinozaki, Scanning squid microscope study of vortex polygons and shells in weak-pinning disks of an amorphous superconducting film, Phys. Rev. B **82**, 014501 (2010).

[160] M. Fogelström, Structure of the core of magnetic vortices in *d*-wave superconductors with a subdominant triplet pairing mechanism, Phys. Rev. B **84**, 064530 (2011).

[161] J. A. Bert, B. Kalisky, C. Bell, M. Kim, Y. Hikita, H. Y. Hwang, and K. A. Moler, Direct imaging of the coexistence of ferromagnetism and superconductivity at the $LaAlO_3$/$SrTiO_3$ interface, Nat. Phys. **7**, 767 (2011).

[162] J. Alicea, New directions in the pursuit of Majorana fermions in solid state systems, Rep. Prog. Phys. **75**, 076501 (2012).

[163] D. Vasyukov, Y. Anahory, L. Embon, D. Halbertal, J. Cuppens, L. Neeman, A. Finkler, Y. Segev, Y. Myasoedov, M. L. Rappaport *et al.*, A scanning superconducting quantum interference device with single electron spin sensitivity, Nat. Nanotechnol. **8**, 639 (2013).

[164] P. J. Curran, S. J. Bending, W. M. Desoky, A. S. Gibbs, S. L. Lee, and A. P. Mackenzie, Search for spontaneous edge currents and vortex imaging in Sr_2RuO_4 mesostructures, Phys. Rev. B **89**, 144504 (2014).

[165] D. Roditchev, C. Brun, L. Serrier-Garcia, J. C. Cuevas, V. H. L. Bessa, M. V. Milošević, F. Debontridder, V. Stolyarov, and T. Cren, Direct observation of Josephson vortex cores, Nat. Phys. **11**, 332 (2015).

[166] P. Holmvall, Modeling mesoscopic unconventional superconductors, Licentiate thesis, Chalmers University of Technology, 2017.

[167] J.-Y. Ge, V. N. Gladilin, J. Tempere, V. S. Zharinov, J. Van de Vondel, J. T. Devreese, and V. V. Moshchalkov, Direct visualization of vortex ice in a nanostructured superconductor, Phys. Rev. B **96**, 134515 (2017).

[168] P. Virtanen, A. Vargunin, and M. Silaev, Quasiclassical free energy of superconductors: Disorder-driven first-order phase transition in superconductor/ferromagnetic-insulator bilayers, Phys. Rev. B **101**, 094507 (2020).

[169] E. Persky, I. Sochnikov, and B. Kalisky, Studying quantum materials with scanning squid microscopy, Annu. Rev. Condens. Matter Phys. **13**, 385 (2022).